ISSN/0393-3016

S. PARRACINO
ENEA guest, Department of Industrial Engineering
University of Rome "Tor Vergata", Rome, Italy

S. SANTORO
ENEA guest, Department of Earth and Sea Sciences
University of Palermo, Palermo, Italy

E. DI FERDINANDO
Nuclear Fusion and Safety Technologies Department
ENEA, Frascati, Italy

G. MAIO
ENEA guest, ARES Consortium, Rome, Italy
present affiliation: Vitrociset SpA, Rome, Italy

M. NUVOLI
Nuclear Fusion and Safety Technologies Department
ENEA, Frascati, Italy

A. AIUPPA
Department of Earth and Sea Sciences
University of Palermo, Palermo, Italy

L. FIORANI
Nuclear Fusion and Safety Technologies Department
ENEA, Frascati, Italy

LIDAR DETECTION OF CARBON DIOXIDE AS A PRECURSOR TO VOLCANIC ERUPTIONS: FIRST RESULTS OF THE CAMPAIGN AT MOUNT ETNA

RT/2016/41/ENEA

ITALIAN NATIONAL AGENCY FOR NEW TECHNOLOGIES,
ENERGY AND SUSTAINABLE ECONOMIC DEVELOPMENT

S. PARRACINO

ENEA guest, Department of Industrial Engineering
University of Rome "Tor Vergata", Rome, Italy

S. SANTORO

ENEA guest, Department of Earth and Sea Sciences
University of Palermo, Palermo, Italy

E. DI FERDINANDO

Nuclear Fusion and Safety Technologies Department
ENEA, Frascati, Italy

G. MAIO

ENEA guest, ARES Consortium, Rome, Italy
present affiliation: Vitrociset SpA, Rome, Italy

M. NUVOLI

Nuclear Fusion and Safety Technologies Department
ENEA, Frascati, Italy

A. AIUPPA

Department of Earth and Sea Sciences
University of Palermo, Palermo, Italy

L. FIORANI

Nuclear Fusion and Safety Technologies Department
ENEA, Frascati, Italy

LIDAR DETECTION OF CARBON DIOXIDE AS A PRECURSOR TO VOLCANIC ERUPTIONS: FIRST RESULTS OF THE CAMPAIGN AT MOUNT ETNA

RT/2016/41/ENEA

ITALIAN NATIONAL AGENCY FOR NEW TECHNOLOGIES,
ENERGY AND SUSTAINABLE ECONOMIC DEVELOPMENT

LIDAR DETECTION OF CARBON DIOXIDE AS A PRECURSOR TO VOLCANIC ERUPTIONS: FIRST RESULTS OF THE CAMPAIGN AT MOUNT ETNA

S. Parracino, S. Santoro, E. Di Ferdinando, G. Maio, M. Nuvoli, A. Aiuppa, L. Fiorani

Abstract

Thanks to the innovative, laser-based, remote sensing system, named BILLI – Bridge Volcanic LIDAR, developed at ENEA (RC of Frascati) by FSN-TECFIS-DIM research group, it has been possible to carry out an experimental campaign at the Mount Etna volcano (CT), from the 28th of July to the 1st of August, 2016. The main goal was to detect the exceedance of in-plume CO_2 concentration, for early warning of volcanic eruptions.
The research is funded by the ERC project BRIDGE – Bridging the gap between gas emissions and geophysical observations at active volcanoes.

Keywords: *Volcanic hazard, Gas detection, Laser remote sensing, Differential absorption lidar*

Riassunto

Grazie al nuovo sistema di telerilevamento ambientale BILLI – Bridge Volcanic LIDAR, messo a punto dal gruppo di ricerca FSN-TECFIS-DIM dell'ENEA (CR Frascati), è stato possibile condurre una campagna sperimentale presso l'Etna (CT) – dal 28 Luglio al 1 Agosto 2016, allo scopo di rilevare la concentrazione di CO_2 presente in eccesso all'interno del plume vulcanico, per fornire un'allerta precoce in caso di eruzione.
Tale ricerca rientra nel progetto BRIDGE - Bridging the gap between gas emissions and geophysical observations at active volcanoes (progetto patrocinato dall'European Research Council).

Parole chiave: Rischio vulcanico, Rivelazione di gas, Telerilevamento laser, Lidar ad assorbimento differenziale

INDEX

1. Introduction

Millions of people currently live in the proximity of active or quiescent volcanoes and, therefore, are potentially exposed to the deleterious effects of their eruptions. In fact, volcanic eruptions can determine an increasing of air pollution levels; they are able to influence climate changes [1] and, in some circumstances, to kill large number of humans, destroying the adjacent environment and causing serious damages to national/international economies.

Mitigation of these effects requires careful assessment of volcano behavior and activity state, which can be accomplished via instrument-based volcano monitoring. Accurate knowledge of gas composition in volcanic plumes gives information on the geophysical processes, taking place inside volcanoes, and provides alert on possible eruptions [2].

Until recently, coupled gas-geophysical studies were sparse, due to the difference in their sampling frequency (low for gas data). This explains the interest of earth scientists in new techniques of gas detection, in particular for CO_2, the second most abundant gas in volcanic fluids and the most directly linked to "pre-eruptive" degassing processes [2].

In the last 30 years, several ground based optical sensing systems have been developed [3] for sounding volcanic particulate in the troposphere [4], in the stratosphere [5], for monitoring fluxes of aerosol [6], SO_2 [7,8] and H_2O [9] in volcanic plumes. However, the scarcity of volcanic CO_2 flux data in the geological literature (see Burton et al. 2013 [10] for a recent review) is a direct consequence of the technical challenges in resolving the volcanic CO_2 signal from the large atmospheric background (≈ 400 ppmv) [11].

In order to fill this gap, a new Differential Absorption Lidar (DIAL), designed to measure the volcanic CO_2 flux, was developed as part of the ERC Starting Grant Project "BRIDGE". The BrIdge voLcanic Lidar (BILLI), recently assembled at ENEA Research Center of Frascati, successfully retrieved three-dimensional tomographies of volcanic CO_2 in the plumes, at Italian volcanoes Pozzuoli Solfatara (Naples, Italy) [12,13,14], and Stromboli volcano (Sicily, Italy) [11,15,16]. To our knowledge, this was the first time that a lidar system retrieved range-resolved measures of both CO_2 concentration and flux in a volcanic plume.

BILLI has opened unprecedented possibilities in measuring volcanic CO_2: an excess of a few tens of ppm could be clearly resolved beyond 3 Km of distance, with spatial resolution of 5 m and temporal resolution of 10 s [15].

Quantifying the CO_2 output from Pozzuoli Solfatara and Stromboli was vital to interpreting – and possibly predicting – the future evolution of the volcanic system, with huge benefit of the population living nearby. These examples show the huge social values of lidar systems in monitoring gas emissions. Observations at densely populated volcanic regions will have a high societal impact throughout Europe.

The final experimental campaign, to test our system performance, has been carried out between the July and the August of 2016 at the Mount Etna (CT), the largest and most important volcano in Italy and one of the most active volcanoes in the world [17]. In this regard, both the setup of the system and the data processing routine have been maintained. Furthermore, thanks to a better wavelength setting, due to the implementation of a photo-acoustic cell, and an appropriate laser-telescope alignment, the measurement error has been

reduced. As it will be showed in the following, these facts have slightly improved the accuracy of our measurements.

Similarly to the previous campaigns, the main goal of this latter one was to measure the exceedance of in-plume CO_2 concentration, so as to provide useful information to volcanology research, for a precocious alert to population in case of eruptions.

For these reasons, this report has to be considered as an extension of the previous works [15,16]. In fact, here the attention will be primarily focused on successful results, concerning CO_2 plume retrieved beyond 4 Km, the longest optical path ever reached by our system.

A brief description of BILLI system and the newly designed BRIDGE DIAL data processing technique will be shown, respectively, in Section 2.1 and 2.2. Moreover, an overview about the experimental setup of the system and the meteorological conditions, during the measurement sessions, will be reported in Section 3. Finally, a fully comprehensive analysis of the field operations and, in particular, of CO_2 profiles and dispersion maps, achieved by Matlab routines, will be discussed in Section 4.

2. Materials and methods

2.1 The BILLI system

BILLI [15] is a complex DIAL system for environmental remote sensing that provides ground based and range resolved remote measurements.

It is mounted in a truck, usually positioned far from the volcanic plume and probes it with its laser beam. Thanks to two large elliptical mirrors the instrument field of view – FOV can be aimed to any direction. With such configuration, and scanning the plume in both horizontal and vertical planes, the CO_2 concentration outside and inside the volcanic plume is measured. These measurements, once carried out over a significant part of the plume, and upon scaling to the transport rate (as derived from the wind speed at the plume altitude), allow one to retrieve the carbon dioxide flux. More details about this procedure are reported in Ref. 11, 14 and 15.

The system is composed of a transmitter and receiver equipment (visible in Fig. 1a). Instead, a particular of the telescope mirrors are visible in Fig. 1b.

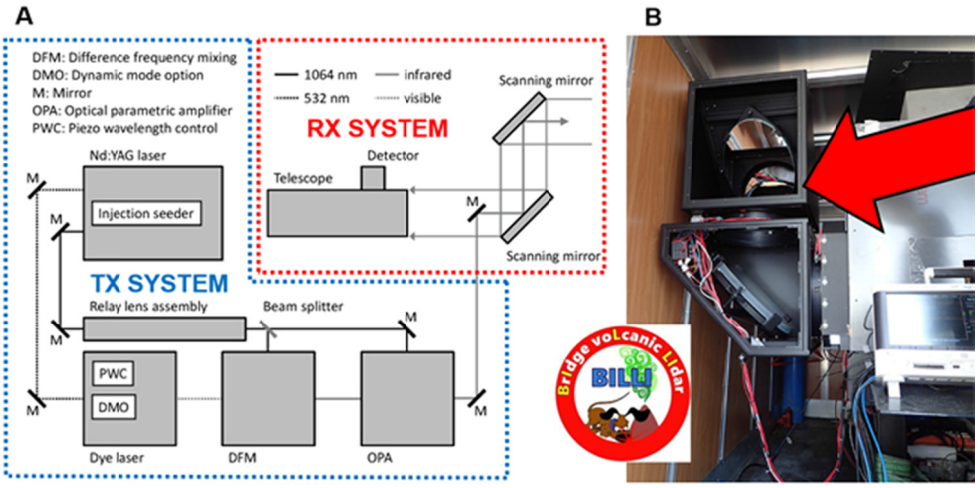

Fig. 1 Technical scheme of BILLI system (A). The red arrow indicates the two large elliptical mirror inside their precision motorized turning mount (opened) (B). The box behind the arrow contains lasers and telescope.

The transmission sub-system is based on: a double grating dye-laser optically pumped by an injection seeded Nd:YAG laser (powerful, tunable and narrow-linewidth), a device for the frequency duplication (DFM – Difference Frequency Mixing) and an Optical Parametric Amplifier operating in NIR band (OPANIR). Tm, Ho:YLF and fiber lasers have been discarded mainly for their limited tunability (few tenths of nm) that can prevent to choose the best absorption line. OPO (optical parametric amplifier) could also be a good choice, but our experience shows that they tend to be quite delicate and not easy to deploy in the harsh environment near degassing craters [15].

Instead, the receiver sub-system is based on: a telescope, a detector and an analogical to digital converter (ADC). More details concerning the mode of operation of the BILLI system are reported in previous works [11-16]. The specifications of the whole system are reported in Table 1 [15].

Transmitter	Pulse energy	25 mJ
	Pulse duration	8 ns
	Repetition rate	10 Hz
	Wavelengths	ON: 2009.537 nm, OFF: 2008.484 nm
	Laser linewidth	0.04 cm^{-1}
	Beam divergence	0.5 mrad
Receiver	Mirror coating	Al
	Clear aperture	300 mm
	Focal length	900 mm
Scanning elliptical mirrors	Mirror coating	Al
	Clear aperture	320 mm x 451 mm
Detector module	Photodiode	InGaAs PIN
	Diameter	1 mm
	Responsivity	1.2 $A \cdot W^{-1}$
	Gain	5.1 9 104 $V \cdot A^{-1}$
	Noise equivalent power	10 pW $Hz^{-1/2}$
	Bandwidth	0–10 MHz
Analog-to-digital converter (ADC)	Dynamic range	14 bit
	Sampling rate	100 $MS \cdot s^{-1}$

Table 1 Main specifications of the BILLI DIAL system during the Mount Etna volcano field campaign.

It is well known that CO_2 absorbs in the 15, 4.2, 2.1 and 1.6 μm bands (in order of decreasing strength) [13]. Unfortunately, in the first two bands viable lasers are not available and atmospheric backscattering is rather low, so the 2.1 band has been chosen for its detection [15]. Nevertheless, the DIAL measurement of CO_2 remains a difficult task because the absorption lines are narrow and weak [13]. Furthermore, with respect to Pozzuoli Solfatara field campaign [12,13,14], the operative wavelengths have been slightly changed (see Table 1). In order to reduce the differential absorption cross section of carbon dioxide ($\Delta\sigma$), thus allowing the laser beam to reach longer ranges.

Summarizing, the main characteristics of the BILLI DIAL system are the following:

- the system is able to explore the atmosphere in both vertical and horizontal directions;
- each lidar profile is obtained averaging 50 shots ON and OFF (interlaced between them with t_{shift} = 0.1 s);
- the temporal resolution between laser shots (Δt) is equal to 10 ns, corresponding to ΔR of 1.5 m;
- a concentration profile is obtained (≈ 40 s) by a couple of lidar signals (ON and OFF) using the newly designed mathematical technique explicitly developed for this application;
- starting from lidar signals of the same scan it is possible to retrieve the dispersion map of in-plume CO_2 concentration [ppm] in the investigated area;
- knowing the (estimated) plume speed it is possible to obtain the CO_2 flux [Kg/s];
- starting from lidar profiles acquired successively, it is possible to track, as rapidly as possible, the motion of discrete atmospheric particles emitted by the volcanic crater. This allows one to estimate also the wind speed [18].

2.2 The BRIDGE DIAL technique

From the literature [18,19,20], the optical power returned to the lidar receiver at any time t is produced by back-scattering of the laser beam by an atmospheric layer at distance R (range) from the source, where R = ct/2 and c is the speed of light. As such, the lidar offers range-resolved information on atmospheric structure and properties (aerosols, particles and gas molecules) along the laser beam, in the form of intensity vs. range plot.

Generally, raw data are normalized to the laser energy, and the flat baseline of each return, which is proportional to the intensity of background noise, is subtracted. Background noise here is defined as an average of data points sampled at the far end of the signal trace (see Fig. 2a).

Upon its atmospheric propagation, the beam intensity decreases approximately: exponentially, due to atmospheric extinction, according to Lambert-Beer law and as $1/R^2$, because the solid angle subtended by the receiver is A/R^2, where A is the telescope effective area. For these reasons, it is a common practice to use the Range Corrected Signal – RCS for lidar data processing (see Fig. 2b). To improve the signal-to-noise ratio (SNR), 100 laser shots were averaged for each lidar return and a Savitzky-Golay filter [21] algorithm with 13 points was employed (Fig. 2c).

Since the system works in DIAL mode, each intensity profile is acquired at two distinct wavelengths, λ_{ON} – absorbed by CO_2 – and λ_{OFF} – not absorbed by CO_2. The two wavelengths are so close that atmospheric behavior, except from CO_2 absorption, is practically identical. Thanks to the measured intensity contrast, between the co-emitted λ_{ON} and λ_{OFF} signals, and using the BRIDGE DIAL technique [11-16], it is possible to retrieve the range-resolved CO_2 concentration profile in the volcanic plume.

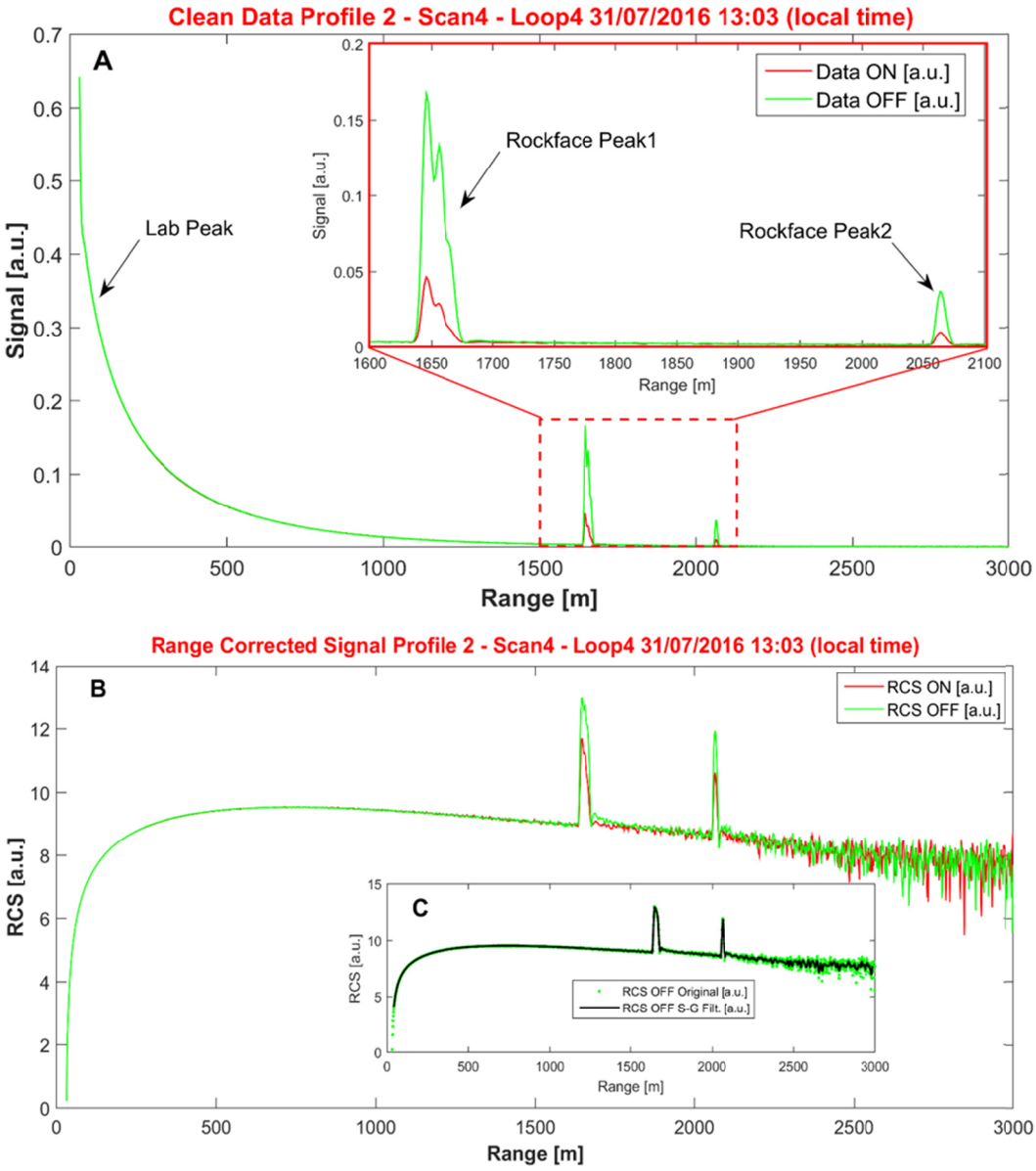

Fig. 2 Example of a lidar profile acquired at 13:03 (local time) of the 31st of July 2016, at an elevation angle of 7.25° and azimuth of 230°. Data profile cleaned by the noise and a magnification of laser beam reflection off Etna rockfaces (A), RCS (B) and filtering of the OFF channel (C).

In order to obtain the results reported in this work, transmitted wavelengths and data processing have been slightly modified with respect to Pozzuoli Solfatara campaign [12,13,14], due to the greater distance of the volcanic plume and the lower concentration of carbon dioxide.

The transmitted wavelengths have been changed (ON: 2009.537 nm, OFF: 2008.484 nm) in order to reduce $\Delta\sigma$, the differential absorption cross section of carbon dioxide, thus allowing the laser beam to reach longer ranges.

Then, we have processed each acquired atmospheric profile using a Matlab analysis routine, with the aim of calculating the CO_2 concentrations in the atmospheric background, and in the volcanic plume. The data processing routine consists of the following steps, all based on the Lambert-Beer law relation:

a) Initially, the CO_2 concentration in the natural background atmosphere, C_0, is calculated as:

$$\ln\left[\frac{I_{P_1,OFF}/I_{0,OFF}}{I_{P_1,ON}/I_{0,ON}}\right] = 2\Delta\sigma\, C_0\, R_{P_1} \tag{1}$$

where: $I_{P1,ON}$ ($I_{P1,OFF}$) stands for intensity of the ON (OFF) lidar signal caused by reflection of the laser beam off the surface of the first wall-rock of the Mount Etna (1600 m<R_{P1}<1700 m, see Fig. 2a); $I_{0,ON}$ ($I_{0,OFF}$) is the intensity of the ON (OFF) lidar peak, caused by laboratory scattering of the laser pulse (see Fig. 2a) and $\Delta\sigma$ is the CO_2 differential absorption cross section;

b) Secondly, ΔC, the average excess CO_2 concentration in the volcanic plume cross-section between the first and second rockface of the Etna, is derived from:

$$\ln\left[\frac{I_{P_2,OFF}/I_{P_1,OFF}}{I_{P_2,ON}/I_{P_1,ON}}\right] = 2\Delta\sigma\left(C_0 + \Delta C\right)\left(R_{P_2} - R_{P_1}\right) \tag{2}$$

where: $I_{P2,ON}$ ($I_{P2,OFF}$) is the peak intensity of the ON (OFF) lidar signal caused by reflection of the laser beam off the surface of the second rock wall of the Etna (2050 m<R_{P2}<2450 m see Fig. 2a);

c) Thirdly, $C_{CO2,i}$, the excess of CO_2 concentration, corresponding to each i-th ADC channel of the lidar profile, is calculated from:

$$C_i = k\, S_i \tag{3}$$

where:

- $k = \dfrac{\Delta C\left(R_{P_2} - R_{P_1}\right)}{\Delta R \sum_i S_i}$ is the multiplication factor;
- $S_i = \ln(I_{i,OFF} R_i^2)$ is the Range Corrected Signal;
- ΔR is the range interval corresponding to an ADC channel;
- $I_{i,OFF}$ is the OFF signal of the i-th ADC channel (the OFF signal has been chosen because of its signal-to-noise ratio is higher);
- R_i is the the range of the i-th ADC channel.

d) the zero level of C_i has been calculated outside the volcanic plume.

e) Finally, the two main error sources, that affected our measurements, have been evaluated:

   i. *systematic error of the CO_2 concentration measurement* – Taking into account of the experience [11,14] the systematic error of our system is dominated by imprecision in wavelength setting [12], leading to inaccuracy in differential absorption cross section and thus in gas concentration. To minimize this error, we implemented a photo-acoustic cell filled with pure CO_2 at atmospheric pressure and temperature, close to the laser exit, in order to control the transmitted wavelength before each atmospheric measurement. This procedure allows to set the ON/OFF wavelengths with better accuracy than the laser linewidth [15]. Assuming that the error in the wavelength setting is ± 0.02 cm^{-1} (half laser linewidth), in the wavelength region used in this study, the systematic error of the CO_2 concentration measurement is 5.5% [11].

   ii. *statistical error of the CO_2 concentration measurement* - The statistical error has been calculated by standard error propagation techniques [22] from the standard deviation of the lidar signal at each ADC channel. In the distance range between the first and the second rockface, representing a mean measurement range, and at typical atmospheric and plume conditions encountered during this study, the statistical error of the CO_2 concentration measurement was about 0.61%.

   Assuming that each error source is statistically independent, we can quadratic sum all the errors and obtain a cumulative error of ~ 6.1% (dominated by the systematic error), a lower value than the previous campaign. In fact, at Stromboli the quadratic sum of same error contributions was about 8% [11].

As already stressed, the repetition rate was 10 Hz and each CO_2 profile was obtained averaging only 100 lidar returns (50 at ON and 50 at OFF), corresponding to an integration time of about 40 s. Plume scans were acquired only along the vertical path and retrieved combining more than 30 profiles, in less than 18 minutes. Typically, 50 scans (or more) at different elevations were repeated, for each measurement day, obtaining three-dimensional tomographies of the volcanic plume.

3. Overview of the experimental campaign

3.1 Experimental setup

The area chosen for our experiments was the summit crater of the Mount Etna volcano (3329 m above the sea level – ASL), that is placed between the province of Messina and Catania, in Sicily (Fig. 3a). This hostile and inhabited region hosts one of the most active volcano in the world. It is characterized by extremes of temperature, high humidity and rates of rainfall, the presence of acid vapors, re-suspended dust and particles, which are toxic for humans and dangerous for the instrumentation [17].

Notwithstanding the harsh environment, BILLI operated practically continuously for nearly a week (from July 28-31, to the 1st of August 2016, including an initial instrumental setup phase), thanks to good weather conditions (see Section 3.2).

During our experiment, the system was placed into a 3.5-ton laboratory truck (Fig. 3b), positioned into the courtyard of INGV observatory, at 2823 m ASL, in the North-East side of the main crater. This fixed position, about 500 m below the volcano's summit, is ≈ 3 Km far from the main degassing vents. This distance guaranteed the safety of operators.

Vertical scans were performed at constant azimuth angle (230°) and at elevation angles from 7° to 14° (Fig. 3c). In such conditions, two rockface peaks were intercepted by laser line of sight (LOS) at elevation angles between 7° and 9°. Carbon dioxide was encountered and measured inside the volcanic plume in the 2.2-4.2 Km range.

Finally, preventive measures have been adopted in the field, in accordance with the European directive 2006/25/EC [23], to ensure that laser beam did not hit buildings (INGV observatory), or persons. In particular, the laser pointing angle was sufficiently high in elevation to avoid this fact. In addition to this, the access to the area just around the system location was restricted, in order to guarantee the access only to authorized personnel that wore protective glasses.

This experimental setup did not affect the use of the laser and, at the same time, guaranteed the safety of operators.

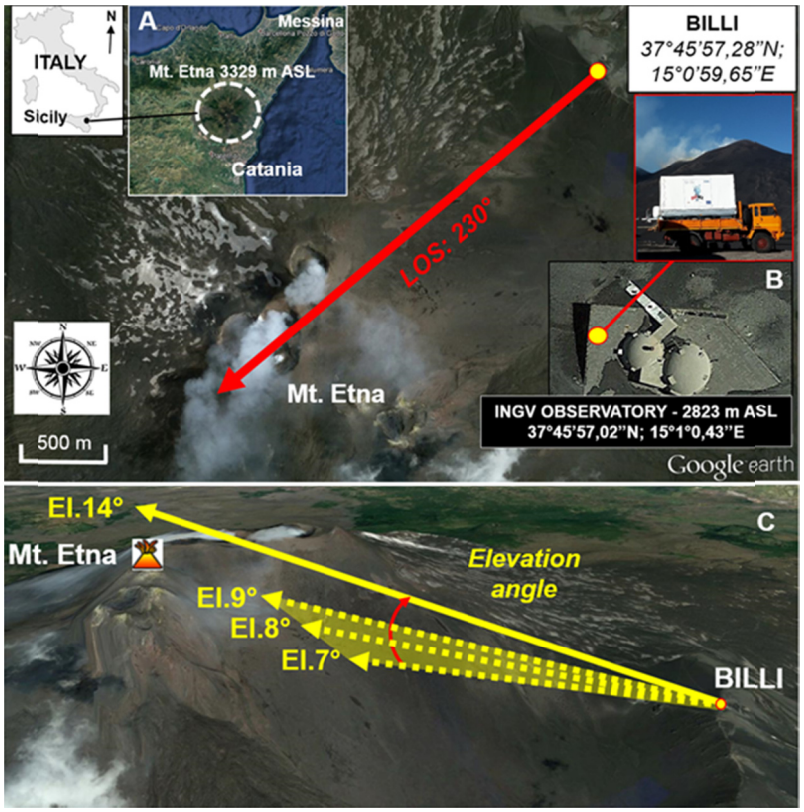

Fig. 3 Experimental area in which the campaign was carried out (A). Geographical coordinates of both the BILLI system and the INGV observatory in which the former was placed (B). The red arrow indicates the azimuth pointing angle of the laser beam (with a fixed line of sight – LOS equal to 230°). The variation of elevation angle (7° to 14°) is showed in (C). Yellow dotted arrows indicate the elevation angles in which the laser beam has intercepted the rockface of the Mount Etna. The subtended area in yellow shows this fact. Instead, the yellow solid arrow indicates an example of elevation angle (of the laser beam), that exceeds the height of the main crater. Therefore, in these specific cases, measures have been performed in the free atmosphere.

3.2 Meteorological parameters

This paragraph reports the trends of the main meteorological parameters, concerning the measurement sessions (28-31/07/2016 and 01/08/2016) of the experimental campaign of Etna.

As it is known, the weather conditions can strongly influence measurements carried out by conventional techniques and, therefore, also by our remote sensing system.

In particular, here the attention is focused on the analysis of the following parameters: Temperature [°C]; Relative Humidity [%]; Precipitations [mm]; Wind Speed [Km/h] and Wind Direction [°].

Even though the experiments were carried out into a hostile place, with temperatures that can strongly vary during the day (from sub-zero values during the night, to 15° at midday) even in the summer; on the basis of in-field inspections, stable weather conditions persisted during the entire measurement window. In fact, the weather was sunny and the total absence of precipitations, have significantly favored in-situ measurements.

In Figure 3, the most important meteorological trends are reported. These parameters have been taken from the weather archive of a popular forecast website [24], during the second half of July 2016. The trends, compared with the ones acquired by in-situ station of Italian Air Force at Etna's northeast crater observatory [25], have confirmed both the results reported in Fig. 4 and in field observations.

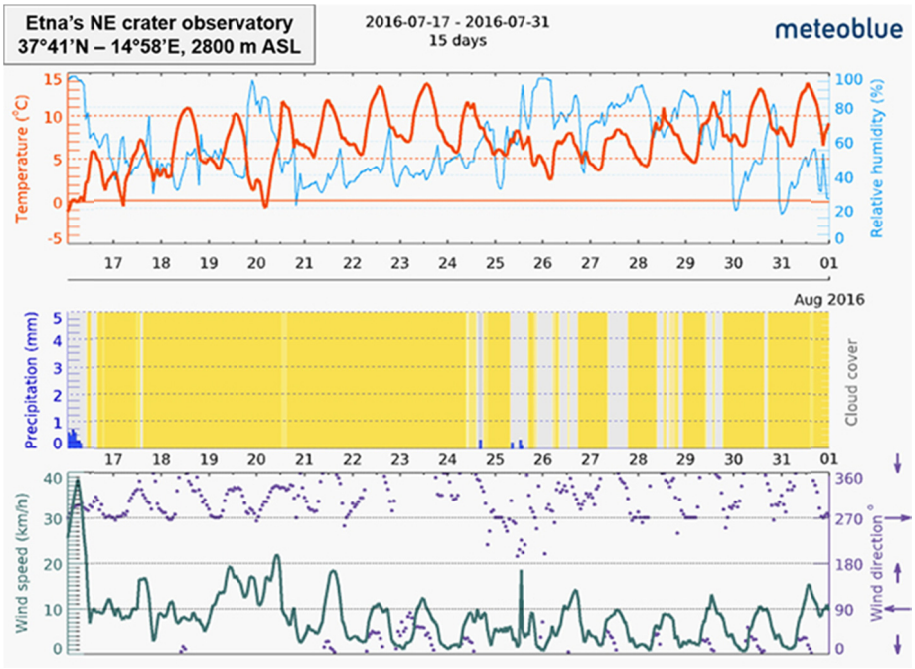

Fig. 4 Meteorological parameters observed at the Mount Etna, during the second half of July, 2016.

In conclusion, weather conditions did not significantly affect BILLI measurements, except for a moderate influence of the wind that blew from North-West and could probably scatter volcanic particles and fumes in the direction of the nearby city of Catania. However, these conditions allowed also a quite good correlation between the detected lidar signals with the data collected by conventional in-situ instruments.

4. Results and discussion

In this section, the results of the Mount Etna field campaign will be presented and thoroughly discussed by means of some useful examples (three significant CO_2 concentration profiles and a series of subsequent dispersion maps) extrapolated from the whole dataset.

As already seen in the Section 2.2, thanks to the BRIDGE DIAL technique, it was possible to retrieve, remotely and in extremely rapid way, the concentration profiles, relative to the exceedance of in-plume CO_2 in the proximity of the main vent of Etna volcano.

Furthermore, after a chronological rearrangement of subsequent profiles, relative to the same vertical scan, it was also possible to draw CO_2 dispersion maps. These tomographies were extremely useful to track the displacements of volcanic plume particles as a function of time, elevation angle and range of acquisition.

During the campaign, it has been noted several configuration of plume that varied as a function of acquisition time. In fact, both the magnitude and the size of CO_2 plume were subject to change with the elevation of the laser beam-pointing angle and, obviously, they were also influenced by the presence of wind.

In general, for elevation angle values comprised within 7° and 9° it was quite common to detect narrow plume peaks attached or strictly close to the first or the second rockface of the Mount Etna. As, for example, for the profile reported in Fig. 5, concerning a signal taken from the Scan n°8, and acquired at 17:27 (local time), with elevation angle equal to 8° and a fixed azimuth (230°).

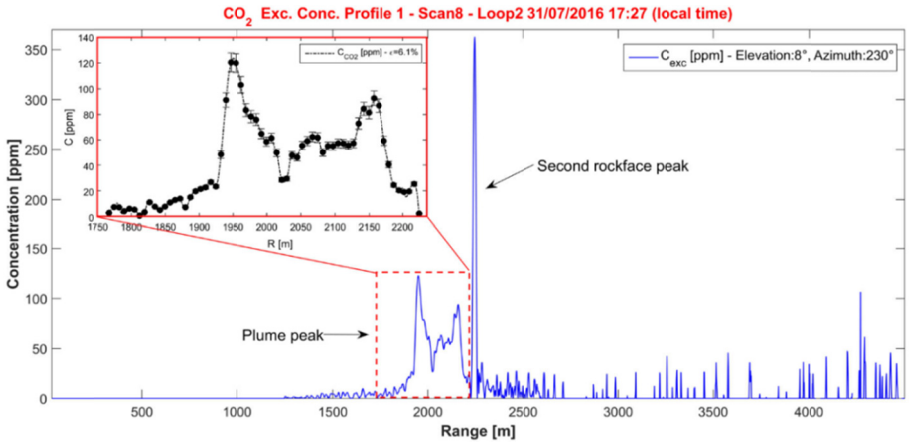

Fig. 5 Example of in-plume CO_2 concentration profile retrieved at the 17:27 (local time). Two peaks are visible, the first one is relative to the presence of plume attached to the second rockface hit by the laser beam (the second peak in the figure). The plume peak has been highlighted into the red dotted box and a magnification of this profile's portion, provided with the y-axis errorbar, is clearly visible in the upper left side of the figure.

In the previous figure, the exceedance of in-plume CO_2 concentration profile shows two peaks, the first one, localized between 1750 and 2230 m (from the system location), is relative to the plume; instead, the second one (placed around 2250 m) is due to the reflection of laser beam to the second rockface. The magnification

of the plume profile (visible in the upper side of the Fig.5) shows also the y-axis errorbar, equal to the 6.1% (see the Sec. 2.2).

Finally, the last portion of the profile (from 2300 m to 4500 m) shows several oscillations, that are due to the residual presence of instrumentation noise. For this reason, the contribution of this segment has been neglected in the following discussion.

The plume reported in the previous figure appears as quite narrow (it extends for about 500 m) and its magnitude does not exceed the value of 140 ppm. It should be noted that at 8° elevation angle, the laser beam altitude was lower than the summit crater one. Therefore, the profiles' behavior could be justified by the proximity of the rockface behind the plume that, de facto, prevented the complete dispersion of the volcanic cloud into the atmosphere and, at the same time, made the wind contribution negligible.

The situation was extremely different by increasing the elevation angle. In fact, it has been noted that the plume tended to disperse and expand more than profiles acquired at lower elevation angles.

Once the laser beam pointing angle exceeded the summit crater, it was possible to notice immediately plume peaks, such as the one reported in Fig. 6 (taken from the Scan n°4 and acquired at 13:08 (local time), at an elevation angle of 9.25°), that was localized around 2.5 Km from the system location.

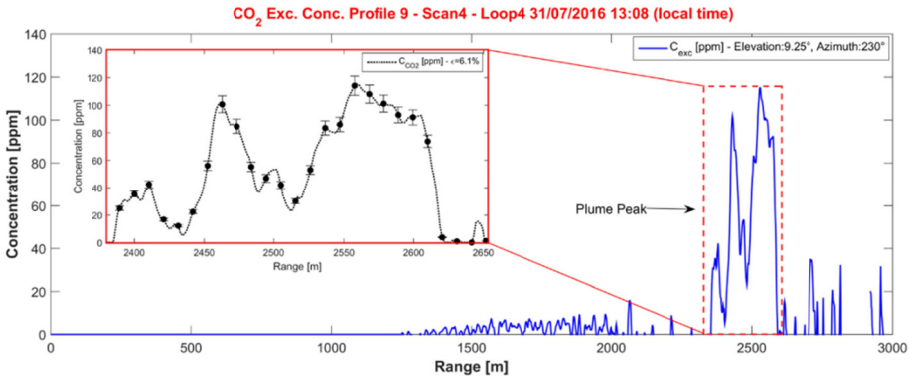

Fig. 6 Example of in-plume CO_2 concentration profile retrieved at the 13:08 (local time). A narrow single plume peak is visible and highlighted into the red dotted box. A magnification of this profile's portion, provided with the y-axis errorbar, is clearly visible in the upper left side of the figure. The same considerations, concerning residual instrumental oscillations, are valid also for this case.

Instead, the concentration profile, reported in Fig. 7, significantly differs from the previous examples, since it has been acquired in the free atmosphere. It concerns a signal taken from the Scan n°6, and acquired at 15:19 (local time), with elevation angle equal to 12° and a fixed azimuth (230°).

It is possible to notice two peaks relative to CO_2 plume highlighted by the red dotted boxes. As we expected from previous considerations, the first peak, localized between 1250 m and 2550 m, and identified by the letter A in Fig.7, is extremely wide (it extends for more than 1 Km) and its magnitude exceeds the value of 150 ppm.

Instead, the second plume peak, around 250 ppm, is identified by the letter B in Fig.7. It has been detected beyond 4 Km (precisely from 4060 m to 4140 m) from the system location and represents the farthest plume

peak ever detected by our system. The magnifications of both plumes, provided with the y-axis errorbar (6.1%), are clearly visible in the lower part of the Fig.7.

Similarly to the previous example, the portion of the profile between the two mentioned plume peaks shows several oscillations. These latter are due to the residual presence of instrumentation noise (see Fig.7). For this reason, it was considered to be negligible.

The behavior of this plume could be justified by the fact that, for such elevation angles and altitudes, the plume was completely dispersed in the free atmosphere and scattered by a moderate presence of the wind (as shown in Section 3.2).

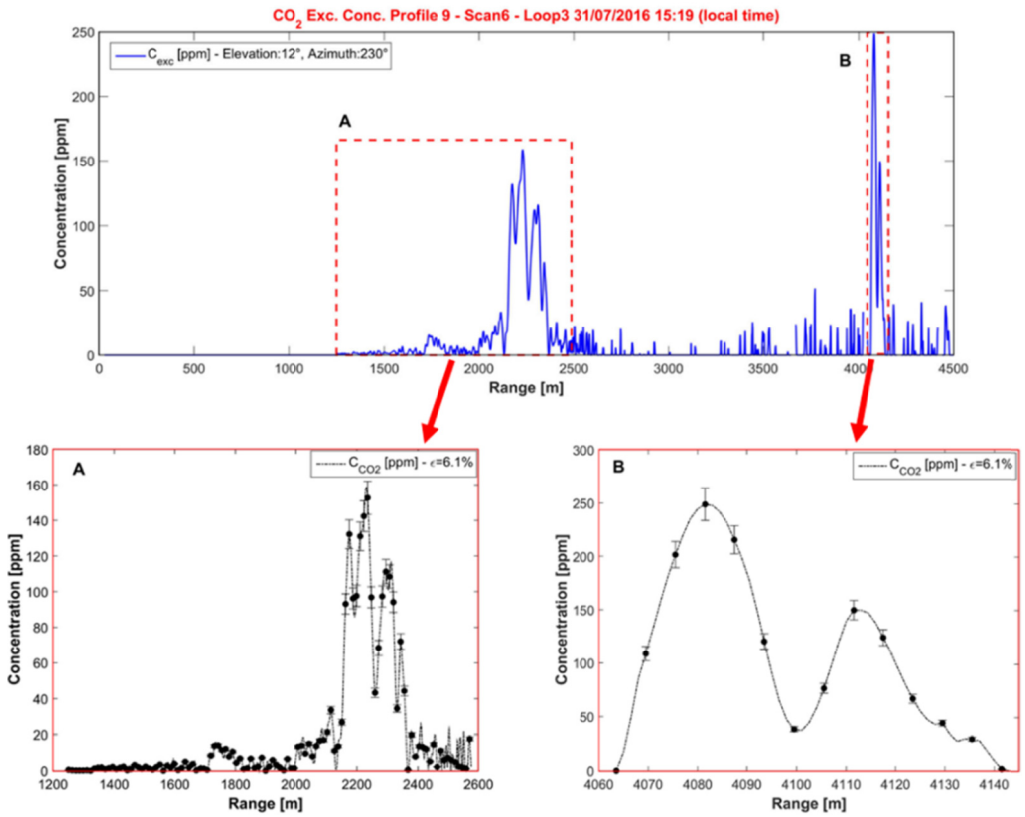

Fig. 7 Example of in-plume CO_2 concentration profile retrieved at the 15:19 (local time). Two plume are visible and they are indicated, respectively, with the letters (A) and (B). Rapid signal fluctuations, between the two mentioned peaks, have been interpreted as the background noise. In the lower part of the figure, it is possible to notice a profile's zoom with the errorbar (uncertainty is equal to 6.1%). The first peak (A) has been detected at 2250 m. Instead, the second peak (B), beyond the 4 Km from the system location.

Finally, Figures 8, 9, 10 and 11 reports 15 examples of CO_2 dispersion vertical maps, acquired successively between 13:20 and 18:15 (local time), during the measurement session of the 31st of July, 2016. This time slot has been selected for the relevance of the results. Each of these tomographies represents the in-plume concentration exceedance as a function of elevation angle and range of acquisition.

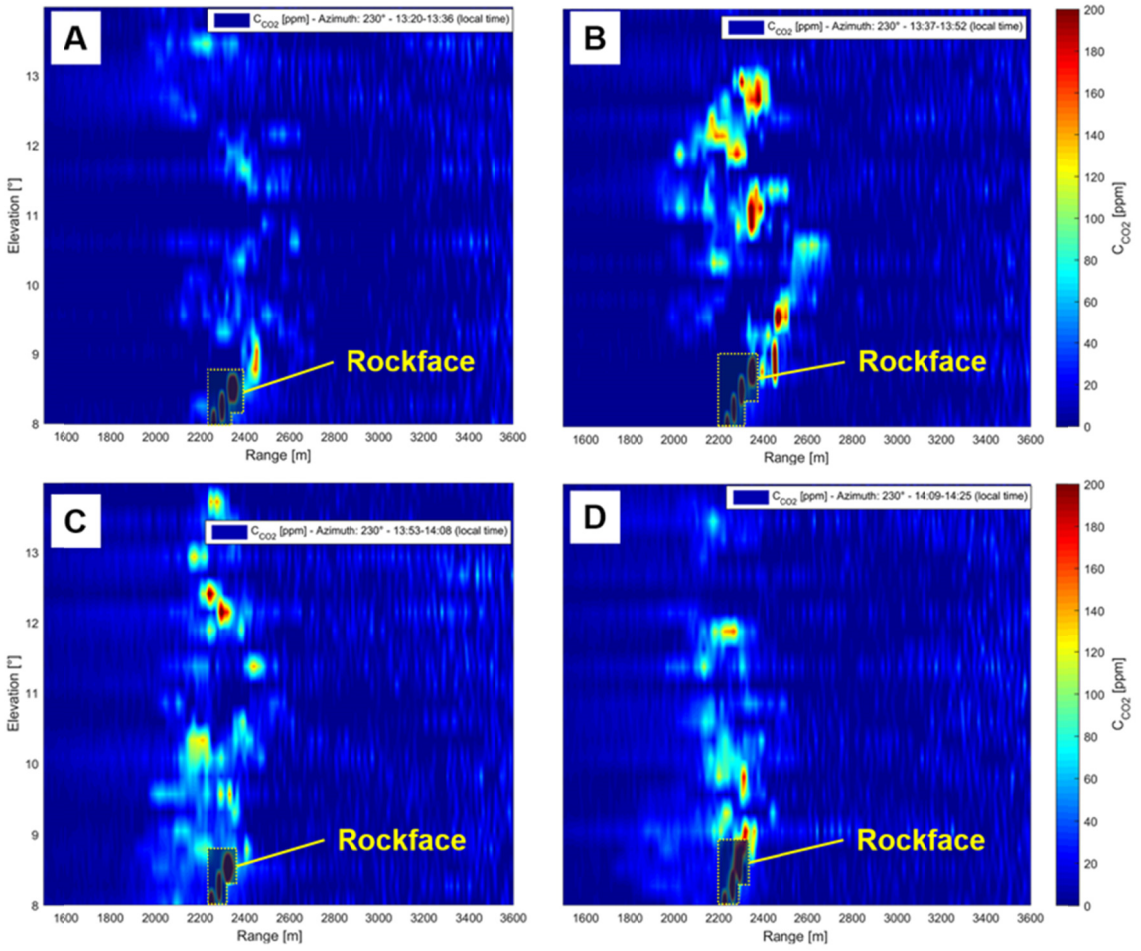

Fig. 8 Exceedance of CO_2 concentration dispersion maps acquired, successively, from the 13:20 to the 14:25 (local time) on July 31, 2016, during the Scan number 5.

This session was composed of 4 vertical loop, each covering about 16 minutes. Each loop consisted of 24 profiles.

The elevation angle was between 8° and 14°. Globally, the system FOV was equal to 6°, with an angular resolution of about 0.25°.

The maximum operative range here was equal to 3.755 Km. Missing and/or erroneous acquisitions between data sets were discarded.

A fixed azimuth angle (230°) was used during the entire measurement session.

It is possible to notice the temporal evolution of the plume (highlighted by red, orange, yellow and green spots) as a function of elevation angle and the range of acquisition. Areas highlighted with yellow dotted boxes indicate the laser beam reflecting off the rockface of the volcano.

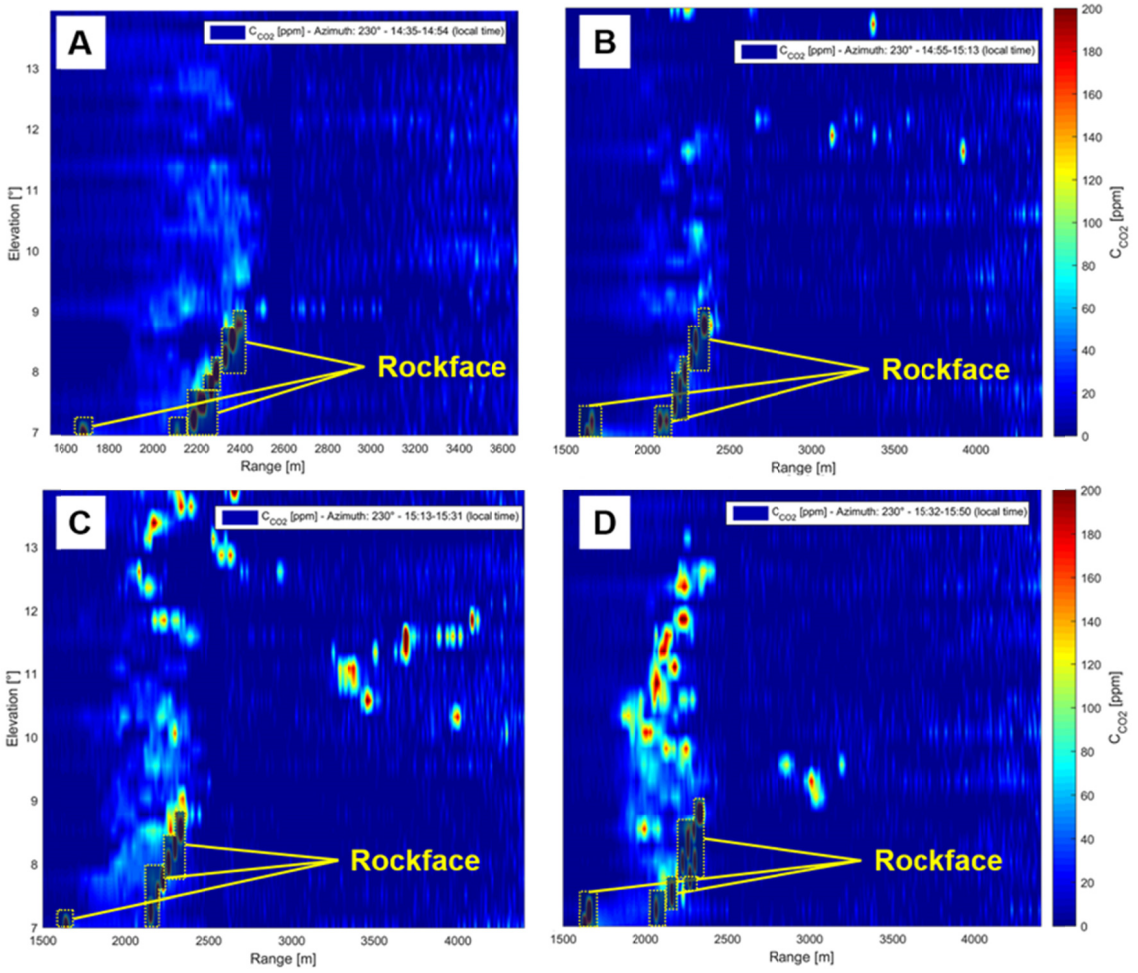

Fig. 9 Exceedance of CO_2 concentration dispersion maps acquired, successively, from the 14:35 to the 15:50 (local time) on July 31, 2016, during the Scan number 6.

This session was composed of 4 vertical loop, each covering about 18 minutes. Each loop consisted of 28 profiles.

The elevation angle was between 7° and 14°. Globally, the system FOV was equal to 7°, with an angular resolution of about 0.25°.

The maximum operative range here was equal to 4.5 Km. Missing and/or erroneous acquisitions between data sets were discarded.

A fixed azimuth angle (230°) was used during the entire measurement session.

It is possible to notice the temporal evolution of the plume (highlighted by red, orange, yellow and green spotss) as a function of elevation angle and the range of acquisition. Areas highlighted with yellow dotted boxes indicate the laser beam reflecting off the rockface of the volcano.

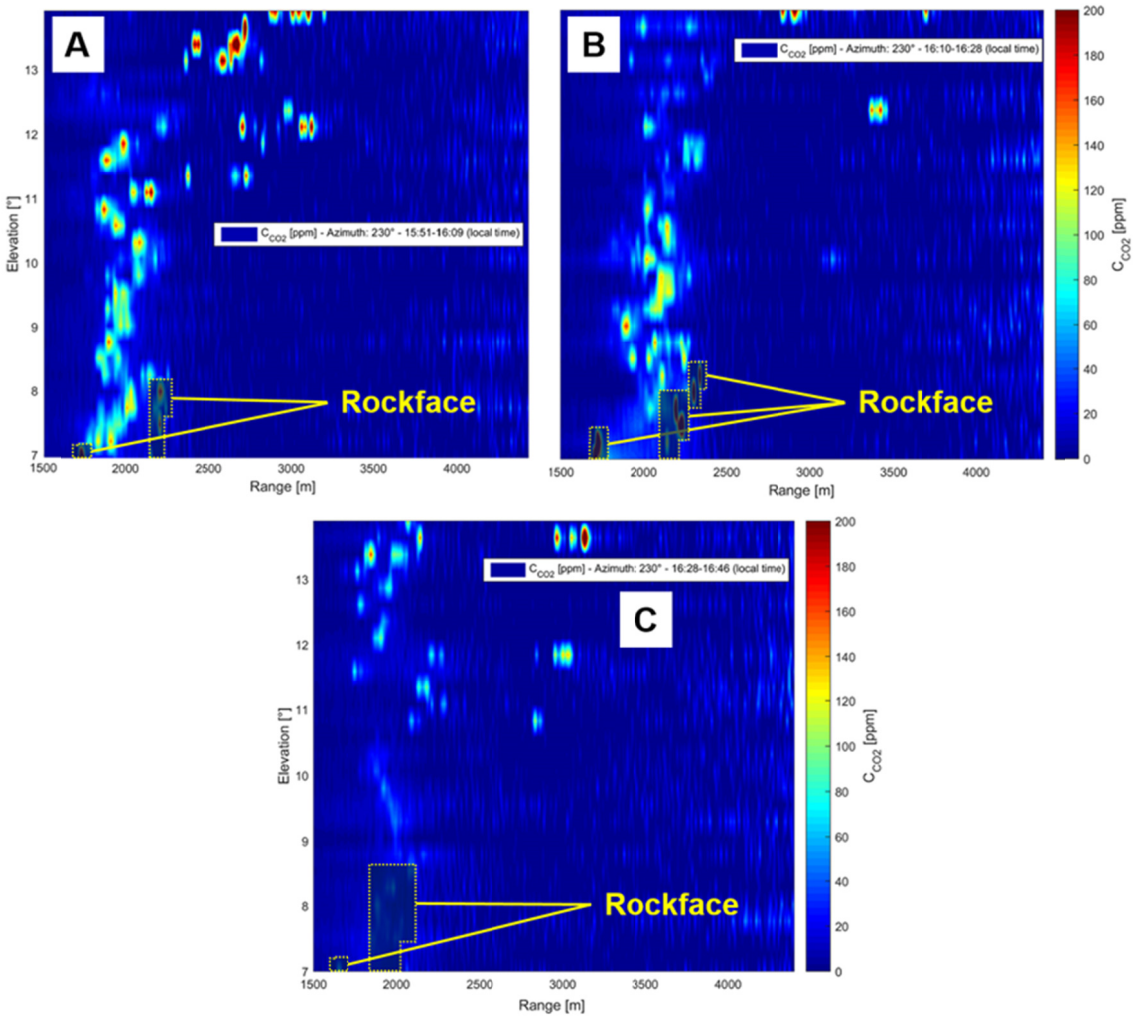

Fig. 10 Exceedance of CO_2 concentration dispersion maps acquired, successively, from the 15:51 to the 16:46 (local time) on July 31, 2016, during the Scan number 7.

This session was composed of 4 vertical loop, each covering about 18 minutes. The last loop was discarded, since it was affected by an unexpected measurement error. Each loop consisted of 28 profiles.

The elevation angle was between 7° and 14°. Globally, the system FOV was equal to 7°, with an angular resolution of about 0.25°.

The maximum operative range here was equal to 4.5 Km. Missing and/or erroneous acquisitions between data sets were discarded.

A fixed azimuth angle (230°) was used during the entire measurement session.

It is possible to notice the temporal evolution of the plume (highlighted by red, orange, yellow and green dots) as a function of elevation angle and the range of acquisition. Areas highlighted with yellow dotted boxes indicate the laser beam reflecting off the rockface of the volcano.

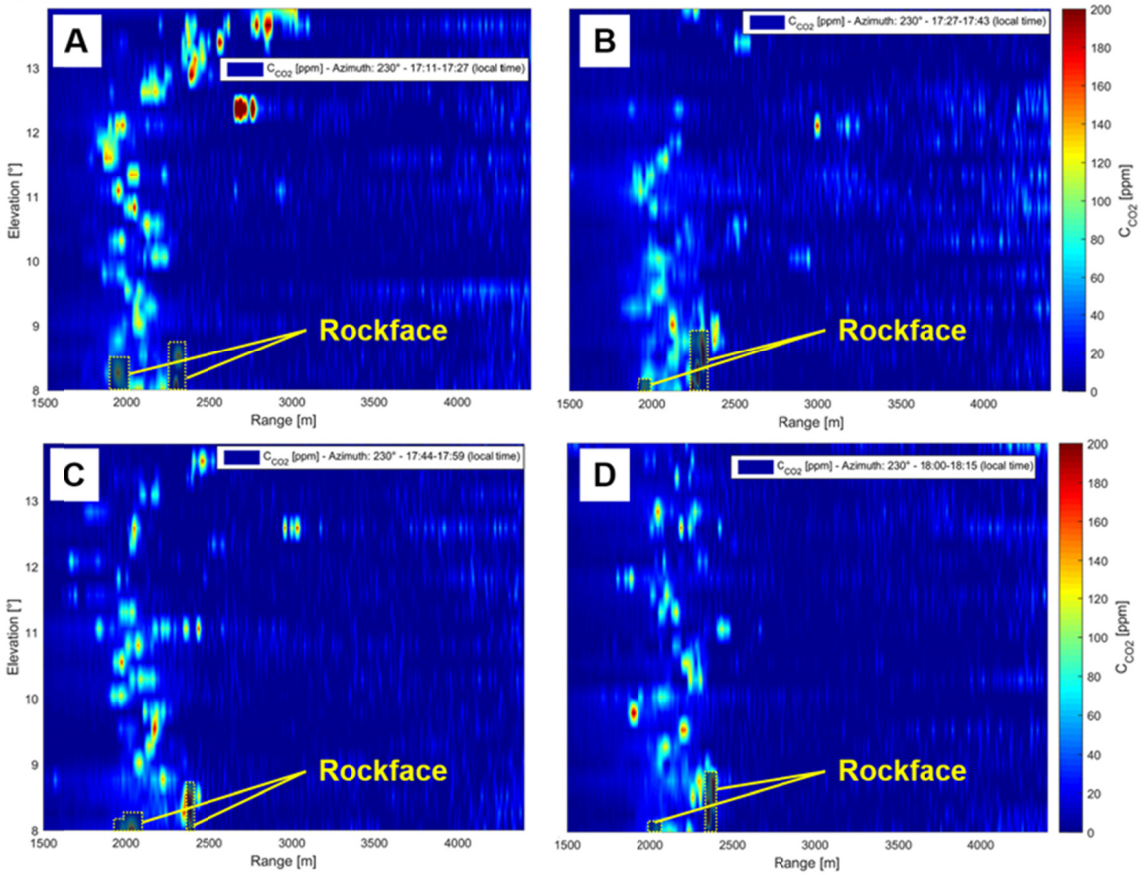

Fig. 11 Exceedance of CO_2 concentration dispersion maps acquired, successively, from the 15:51 to the 16:46 (local time) on July 31, 2016, during the Scan number 8.

This session was composed of 4 vertical loop, each covering about 16 minutes. Each loop consisted of 24 profiles.

The elevation angle was between 8° and 14°. Globally, the system FOV was equal to 6°, with an angular resolution of about 0.25°.

The maximum operative range here was equal to 4.5 Km. Missing and/or erroneous acquisitions between data sets were discarded.

A fixed azimuth angle (230°) was used during the entire measurement session.

It is possible to notice the temporal evolution of the plume (highlighted by red, orange, yellow and green dots) as a function of elevation angle and the range of acquisition. Areas highlighted with yellow dotted boxes indicate the laser beam reflecting off the rockface of the volcano.

In the previous figures, it is clearly visible the time evolution of plume highlighted by the red, orange, yellow and green spots respect to the dark blue color that, instead, represents the CO_2 concentration natural background.

As already stressed, for lower elevation angle, the plume was circumscribed between the first and second rockface of the Mount Etna encountered by the laser beam. The rockface regions have been highlighted by the yellow dotted boxes in the lower side of each scan. Instead, in the free atmosphere, the smoke plume rose

and developed in both vertical and horizontal direction, covering a wide area, after a complete random dispersion, as in Figures 9b,c, 10, 11a,b,c or remaining rather confined as in Figures 8, 9a, 11d.

Obviously, both spatio-temporal and intensity variations of CO_2 concentration, shown in the previous figures, were strictly linked to the variations of emitted particles and ash during the current volcanic activity.

Plume fluctuations in free atmosphere were also probably due to a combination of the thermal updraft, from the main degassing vents on the volcano's summit, and on a smaller scale, to the presence of North-West wind blowing during the measurement session.

Furthermore, differences between subsequent maps were also probably due to rapid, local and random fluctuations of particles and gases emitted by volcano.

In conclusion, the great novelty, respect to the previous works [15,16], is that our measurements allowed us to locate and track volcanic plumes, beyond 4 Km of distance from the system location. The detected values in excess of CO_2 concentrations were in good agreement both with conventional measurements, carried out in the same time interval, and with the previous lidar ones acquired during the Stromboli campaign [15].

The preliminary results reported in this work can be considered to be extremely promising to validate the reliability and accuracy of the system developed at ENEA. Furthermore, they could represent a further step forward in the ground-based volcano monitoring and volcanology research field.

5. Conclusions

In this work, the results of the experimental campaign carried out between the 28th of July and the 1st of August 2016, at the Mount Etna volcano have been reported. The main goal was to detect and analyze volcanic plumes, in order to measure the exceedance of in-plume CO_2 concentration. This gas is extremely important since, according to volcanologists, it is a precursor of eruptions. For this purpose, BILLI, a DIAL system recently developed at ENEA under the ERC BRIDGE project, was used.

The great novelty/advantage of the measurements reported here is that BILLI allowed measurements to be taken continuously, remotely (more than 4 Km) and, therefore, from a safer location free from risks to which operators are exposed during direct sampling, with much higher temporal (40 s) and spatial (5 m) resolution (the plume was scanned in few minutes rather than over several hours). These performances are adequate to follow the spatiotemporal dynamics of the volcanic plume and can provide, quickly and continuously, reliable data on a key precursor of volcanic eruptions.

In conclusion, the BILLI DIAL system was used to retrieve 3D tomographies of volcanic plumes at Etna volcano. CO_2 excess of a few tens of ppm has been clearly detected remotely and in a few minutes scan. Furthermore, a complete time-resolved plume evolution has been detected in several measurement sessions; this fact could also be useful for the measurement of wind speed.

The lidar measurements of CO_2 were in good agreement with results obtained with conventional techniques, yet based on completely independent and significantly different approaches. This has proven the goodness and the reliability of the system developed by the ENEA.

To our knowledge, this is the first time that a CO_2 peak is retrieved by lidar in a volcanic plume, at a distance that exceeds the 4 Km. This fact demonstrates the high potential of laser remote sensing in volcanological research.

In the near future, it will be desirable to deploy a such established laser-based system, to eruptions forecasting, for prolonged periods. This will allow us to provide useful information to volcanologists, concerning the time evolution of volcanic gases in hazardous regions, working remotely and safely.

Acknowledgements

The authors are grateful to ENEA, in general, and Aldo Pizzuto, Roberta Fantoni and Antonio Palucci, in particular, for constant encouragement.
The support from the ERC project BRIDGE, No. 305377, is gratefully acknowledged.

References

[1] "How do volcanoes affect the climate?," The Guardian, London, UK, 9 February 2011 (accessed 1 September 2016). [https://www.theguardian.com/environment/2011/feb/09/volcanoes-climate]

[2] A. Aiuppa, M. Burton, T. Caltabiano, G. Giudice, S. Guerrieri, M. Liuzzo, F. Murè, and G. Salerno, "Unusually large magmatic CO_2 gas emissions prior to a basaltic paroxysm," *Geophys. Res. Lett.* **37**(17), L17303 (2010) [doi:10.1029/2010GL043837].

[3] C. Oppenheimer and A. McGonigle, "Exploiting ground-based optical sensing technologies for volcanic gas surveillance," *Annals of Geophysics* **47**(4), 1455-1470 (2004).

[4] L. Fiorani, F. Colao and A. Palucci, "Measurement of Mount Etna plume by CO_2-laser-based lidar," *Opt. Lett.* **34**(6), 800-802 (2009).

[5] H. Jäger, "The pinatubo eruption cloud observed by lidar at garmisch-partenkirchen," *Geophys. Res. Lett.* **19**(2), 191-194 (1992).

[6] J. N. Porter et al., "Sun photometer and lidar measurements of the plume from the Hawaii Kilauea Volcano Pu'u O'o vent: Aerosol flux and SO2 lifetime," *Geophys. Res. Lett.* **29**(16), 30-1 (2002) [doi: 10.1029/2002GL014744].

[7] T. Casadeval et al., "Sulfur Dioxide and Particles in Quiescent Volcanic Plumes From Poàs, Arenal, and Colima Volcanos, Costa Rica and Mexico," *Journal of Geophysical Research* **89**(D6), 9633-9641 (1984).

[8] P. Weibring, et al., "Monitoring of volcanic sulphur dioxide emissions using differential absorption lidar (DIAL), differential optical absorption spectroscopy (DOAS), and correlation spectroscopy (COSPEC)," *Appl. Phys. B* **67**(4), 419-426 (1998).

[9] L. Fiorani, F. Colao, A. Palucci, D. Poreh, A. Aiuppa, and G. Giudice, "First-time lidar measurement of water vapor flux in a volcanic plume," *Opt. Commun.* **284**(2011), 1295-1298 (2011).

[10] M.R. Burton, G.M. Sawyer and D. Granieri, "Deep Carbon Emissions from Volcanoes," *Rev. Mineral. Geochem.* **75**(1), 323-354 (2013).

[11] A. Aiuppa, L. Fiorani, S. Santoro, S. Parracino, R. D'Aleo, M. Liuzzo, G. Maio and M. Nuvoli, "Frontiers in Dial-Lidar-based remote sensing of the volcanic CO_2 flux," *Frontiers in Earth Sciences – Volcanology* 2016 (submitted).

[12] L. Fiorani, S. Santoro, S. Parracino, M. Nuvoli, C. Minopoli and A. Aiuppa, "Volcanic CO_2 detection with a DFM/OPA-based Lidar," *Optics Letters* **40**(6), 1034-1036 (2015) [doi:10.1364/OL.40.001034].

[13] L. Fiorani, S. Santoro, S. Parracino, I. Maio, M. Del Franco and A. Aiuppa, "Lidar detection of carbon dioxide in volcanic plumes," *Proc. SPIE* **9535**, *Third International Conference on Remote Sensing and Geoinformation of the Environment* (RSCy2015), 95350N, 1-6 (2015) [doi:10.1117/12.2192724].

[14] A. Aiuppa, L. Fiorani, S. Santoro, S. Parracino, M. Nuvoli, G. Chiodini, C. Minopoli, G. Tamburello, "New ground-based Lidar enables volcanic CO_2 flux measurements," *Scientific Reports* **5**(13614), 1-12 (2015) [doi:10.1038/srep13614].

[15] L. Fiorani, S. Santoro, S. Parracino, G. Maio, M. Nuvoli, A. Aiuppa, "Early detection of volcanic hazard by Lidar measurement of carbon dioxide," *Natural Hazards* **83**(21), 1-9 (2016) [doi:10.1007/s11069-016-2209-0].

[16] S. Parracino, S. Santoro, G. Maio, M. Nuvoli, A. Aiuppa and L. Fiorani, "Lidar campaign at Stromboli volcano: methodology and results," *ENEA Technical Report* RT/2016/31/ENEA (2016).

[17] A. Bonaccorso, S. Calvari, M. Coltelli, C. Del Negro, S. Falsaperla, *Mt. Etna: Volcano Laboratory*, Published by the American Geophysical Union as part of the Geophysical Monograph Series, Volume 143. Wiley Online Library, USA (2013) [doi: 10.1029/GM143].

[18] L. Fiorani, "Environmental Monitoring by Laser Radar," Chap. 4 in *Lasers and Electro-Optics Research at the Cutting Edge*, S. B. Larkin, Eds., pp. 123-175, Nova Science Publishers Inc., New York (2006).

[19] V. Kovalev, W. E. Eichenger, *Elastic Lidar, Theory, Practice and Analysis Methods*, Wiley & Sons, Inc., Hoboken, New Jersey, USA (2004).

[20] C. Weitkamp, *Lidar Range-Resolved Optical Remote Sensing of the Atmosphere*, Springer, NY, USA (2005).

[21] R. W. Schafer, "What Is a Savitzky-Golay Filter?," IEEE Signal Processing Magazine 28(4), 111-117 (2011) [doi:10.1109/MSP.2011.941097].

[22] A. Papoulis, U. Pillai, *Probability, Random Variables and Stochastic Processes,* 4th ed., McGraw-Hill, New York (2002).

[23] European Parliament, Council of the European Union, "Directive 2006/25/EC of the European Parliament and of the Council of 5 April 2006 on the minimum health and safety requirements regarding the exposure of workers to risks arising from physical agents (artificial optical radiation) (19th individual Directive within the meaning of Article 16(1) of Directive 89/391/EEC)," *Off. J. Eur. Union* **L114**, 38–59 (2006).

[24] Weather archive of Mount Etna, Meteoblue (accessed 1 September 2016) [https://www.meteoblue.com/it/tempo/previsioni/archive/37.745N14.996E?params=20160731&fcstlength=15]

[25] "Previsioni meteorologiche per Etna-Cratere NE (CT)," Aeronautica Militare, Centro Nazionale di Meteorologia e Climatologia Aeronautica, 26 June 2015 (accessed 31 July 2016) in Italian. [http://www.meteoam.it/ta/previsione/907/etna-cratere_ne]

ENEA
Servizio Promozione e Comunicazione
www.enea.it

Stampa: Laboratorio Tecnografico ENEA - C.R. Frascati
dicembre 2016